International Journal of Environmental Sciences
ISSN: 2229-7359
Vol. 11 No. 10s, 2025
https://theaspd.com/index.php

Modeling And Simulation Of Constrained Predictive Control Systems To Meet Speed Profiles Using Power And Energy Models

[1]**José Luis Sampietro Saquicela**
jose.sampietro@pucese.edu.ec, https://orcid.org/0000-0003-0610-089X, Pontificia Universidad Católica del Ecuador - PUCESE
[2]**Jorge Gabriel Checa Burgos**
jorgecheca@itscv.edu.ec, https://orcid.org/0000-0001-8322-3872, Instituto Superior Tecnológico Ciudad de Valencia, Puebloviejo, Ecuador.
[3]**Raúl Clemente Ulloa de Souza**
raul.ulloa@utelvt.edu.ec, https://orcid.org/0000-0003-1885-0161,Universidad Técnica Luis Vargas Torres de Esmeraldas, Ecuador.
[4]**Jaime Rafael Bastidas Heredia**
jaime.bastidas@eppetroecuador.ec, https://orcid.org/0000-0003-3022-5756, Empresa Pública Estatal Petroecuador, Refinería Estatal Esmeraldas, Ecuador.
[5]**Luz Miriam Ávila Pesántez**
miriam.avila@espoch.edu.ec, https://orcid.org/0000-0001-9421-287X, Escuela Superior Politécnica de Chimborazo, Riobamba, Ecuador.
[6]**Freddy Jeovanny Fares Vargas**
freddyfares@itscv.edu.ec, https://orcid.org/0000-0003-1400-6676, Instituto Superior Tecnológico Ciudad de Valencia, Puebloviejo, Ecuador.
[7]**Leandro Alexander Bermúdez Herrera**
leandro.bermudez@gmail.com, https://orcid.org/0009-0002-3590-7166, Universidad Internacional del Ecuador.

Abstract: *Hybrid electric vehicles (HEVs) are a useful alternative for solving the problems inherent to purely electric vehicles. Among the main problems that are solved is their autonomy. The present work implements a vehicle architecture oriented towards power and energy models, with a fuel cell as the main propulsion element and storage elements such as batteries and supercapacitors. This combination allows the efficient use of energy and power densities, given by the capacities of each of the aforementioned elements. The control system to be implemented is a system based on MPC predictive models, with a variation in the cost function that allows us to control the individual functions by weights. The cost function allows to preserve the useful life of the elements, reduce the efforts of the components for operation in regions of greater efficiency and also weigh the economic operation of each of the elements, regulating their use within the system which can be related to the use of fuel, which in the particular case will be hydrogen. Driving profiles developed for urban service buses are used, and a balance of powers is proposed to meet them, considering the forces contrary to movement, the dissipative forces and the mass of each of the elements.*
Keywords*: Fuel cells, batteries, supercapacitors, predictive control by models.*

1. INTRODUCTION

The growing global demand for energy supply is booming significantly and will continue to increase steadily every day, driven by expanding demographic trends and rapid global modernization that is transforming today's energy landscape. According to the World Energy Outlook (WEO) report, global energy demand is projected to increase by 1% each year at least until 2040 (Solar Energy Management and Sustainability, 2023). It is estimated that total transactional energy consumption increased considerably by 57% between 2002 and 2025, which can explain the emerging need today to develop energy optimization systems by implementing renewable energies. So, in an initial analysis, this scenario strongly argues for the urgent need to increase research on energy issues of great relevance. It is reasonable to say that there are two distinct and different contexts that manifest themselves according to the economic capacities and technological development of the different countries in the world. The first context, which is the majority in third world countries, shows that in these places it is still common to observe that the majority of their electricity generation

and their vehicle fleet is based on technologies that use fossil fuels predominantly. With regard to industrial electricity generation, we find various facilities such as thermal plants, internal combustion engines, gas turbines, nuclear plants, among other alternatives that are used prevalently (Méndez Cruz, 2024). It is common to see centralized architectures implemented based on generators that produce large amounts of energy to be transported through a transmission network to distributors. This type of technology, as expected, presents certain characteristic problems in its operation and maintenance that must be solved effectively. These challenges have led to continuous research and studies to improve all these aspects and ensure their optimal functioning in various situations (Martínez Pérez & Gassinski, 2022; Monterroza-Ríos et al., 2021). Some problems that frequently occur are the amount of methane gas CH4 and carbon monoxide CO emissions, which can significantly affect air quality and contribute negatively to climate change. In addition, the mechanical efficiency of components, such as boilers, generators, and exciters, is critical to ensure optimal system operation, but they often leak over operating time and component wear. It is equally important to consider the performance and efficiency of engines at different points of operation, as this can influence fuel consumption and energy production. Finally, aspects related to torque, power and specific fuel consumption must also be analyzed, which are crucial to optimize the overall performance of the machines and minimize their environmental impact (Cardona et al., 2020).When it comes to classic vehicles, it is essential to address certain issues that directly affect their efficiency and operation. These older cars, which typically feature technology that includes only the injection engine, face several specific challenges. Among the issues that have been studied is the precise amount of air-fuel mixture that is fed into the cylinders, a critical aspect for engine performance. Torque control is also essential, as it allows you to manage the power that is produced and transmitted to the wheels (Lozano, 2024). In addition, the regulation of ignition control is another key factor in maximizing the efficiency of the machine as a whole. It is necessary to prevent unwanted ignition processes from occurring, which can lead to the destruction of pistons and other parts of the cylinder, a situation that can arise as a result of high pressure peaks. Likewise, issues related to the thermal efficiency of the engine must be considered, which directly impact its operation and durability (Gadvay Lara & Monar Arguello, 2021; Rodríguez Tapia & Plasencia Caiza, 2021). All these aspects produce lower efficiency than other types of engines such as electric and fuel cell-based. In relevant academic works such as those of Bedoya Caro et al., (2007); Guzzella & Onder, (2010); Melo Espinosa et al., (2012), a series of inherent and complex problems associated with this type of technology have been extensively addressed, problems that have been mentioned in the previous paragraphs and that belong to what we have defined as the first context of analysis. Currently, various contexts are developing that focus decisively on the transition from the use of fossil fuel-based technologies to clean and renewable energy alternatives. The main problems that do not allow the promotion and sustenance of the growth of renewable energies are multiple and varied. One of the most significant is that the vast majority of the sources that are the basis of today's energy condition are mostly dependent on fossil fuels, which poses a critical challenge for long-term sustainability. This scenario is affected by a number of reasons, including the worrying depletion of fossil fuel reserves, which results in an urgent need to find sustainable solutions. In addition, global warming is a pressing problem that affects the entire planet and is directly related to the intensive use of these polluting technologies. Other issues that should also be considered are those related to efficiency in terms of resource management, energy security and the continuous increase in costs associated with the production and consumption of electricity (Martínez Pérez & Gassinski, 2022).During the transition from the first context to the second, a number of innovative solutions were implemented. One of them was the design and development of vehicles that are lighter and more efficient, capable of operating without the need for high consumption of fossil fuel or electricity. In addition, initiatives were enacted to encourage individual power generation through various plants that use resources such as solar energy, wind energy, or other clean and sustainable generation methods. In the near future, a migration will take place due to the current problems around these solutions and the current trends in technological development and research relevant to the areas of application, both for Electric Vehicles (EVs) and Smart Grids.The problem of energy depletion and environmental pollution has become the main driving force that is essential to effectively address the many environmental challenges we face today. In addition, this transformation is critical to ensuring a sustainable and reliable energy supply for future generations that depend on these resources. In this sense, the integration of advanced technologies, such as predictive control systems, play a crucial role in facilitating the optimization of the use of available energy resources. This is especially relevant in the specific context of HEVs, where the aim is to maximize efficiency. The implementation of these systems allows for more efficient use of batteries and supercapacitors integrated into vehicles, which contributes to drastically reducing energy waste and, at the same time, improving the range of vehicles on the road. Consequently, it can be said that predictive control systems not only play a fundamental role in energy sustainability, but also optimize the overall performance of HEVs, which are increasingly

present in a highly competitive automotive market (Ulutas et al., 2020).This situation is crucial to meet the growing expectations of modern consumers, who are actively looking for vehicles that are not only efficient, but also sustainable. In addition, by integrating advanced technologies such as batteries and supercapacitors, an optimal balance between performance and range is achieved, resulting in a significantly better driving experience. In this broad context, the modelling and simulation of predictive control systems have become essential tools for anticipating and effectively managing energy demand (Barceló Serra, 2023; Bragagnolo et al., 2020). Thus, the problem of energy depletion and environmental pollution remains the main driving force behind the move from the first scenario to the second, as mentioned above. Based on this growing problem, gasoline vehicles are gradually being replaced by a new generation of hybrid or pure electric vehicles, therefore, the main objective of this study is to develop a control system for efficient energy storage using batteries and supercapacitors, and to demonstrate the efficiency of EVs in relation to conventional vehicles. Another significant contribution is the use of the fuel cell also known as the hydrogen engine, replacing the internal combustion engine. Because it produces zero emissions, it has greater efficiency and allows migrating from the first scenario to the second. The combination of these 3 elements ensures that there is proper management of the supercapacitor's power density and the energy density of the batteries. By 2030, approximately 24% of new cars sold in Europe and 12% in the US are expected to be EVs, while 13% and 6% respectively will be purely electric vehicles (Mohamed Khaleel et al., 2024; Sinézio Martins et al., 2024). It is clear that the development of EV control technologies should not only be considered as one of the fundamental research axes, but should also be a priority in the modern automotive industry. The main topics to be addressed in the field of control are EV torque management, which plays a crucial role in EV performance, implementation of efficient EV storage management systems, including batteries and other components, advanced powertrain engineering to optimize energy conversion, and recuperative control optimization, which helps to improve the energy efficiency of vehicles. All this reflects the importance and need to advance in these fields to achieve the sustainability and efficiency objectives that are currently being set (Alvarez Díaz, 2023; Barceló Serra, 2023; García, 2024).This research has been structured in 4 sections. Section 2 provides mathematical models of each of the components, driving profiles and mathematical design of the MPC controller. Section 3 is where the simulations oriented to energy management are found with the operation of the storage components using the predictive control system for each driving profile, with the fuel cell as the main input element. Finally, the conclusions and future work of the study are described in section 4.

2. METHODOLOGY

2.1 Research Overview

In general guidelines, this work will be based on demonstrating the energy management of an EV efficiently through speed profiles. The main source of energy generation will be the hydrogen engine or fuel cell and the chosen storage sources are the battery and the supercapacitor. The architecture of the EVH will be established considering the layout of the topology and the flow of energy between the different elements of the EVH, in such a way that through the BADC and Manhattan speed profiles the performance and efficiency can be evaluated. The MPC controller will allow optimizing system performance in real-time, adjusting control actions based on model predictions. In the context of economic predictive control (EMPC), it is emphasized that the cost function is formulated to optimize the use of resources and minimize operating costs, which is crucial for energy management in HEV. So, MPC control is a variation of the cost function of MPC control. To carry out the research, firstly, the architecture of the HEV was established. Subsequently, the model of each component that makes it up was defined as the model of the battery, the battery, the electric motor and the supercapacitor.

2.2 Vehicle architecture

The architecture of an EV refers to the topological relationship and energy flow between its components (Sabri et al., 2016; Mittal & Shah, 2024). The main configurations are series, parallel and series-parallel. The design and selection of an EV architecture is a critical procedure, as it influences future design, control, and optimization. As a first step, we will define the total power that the vehicle's powertrain components will deliver. Vehicle dynamics are based on the energy balance of the forces that contribute to the vehicle's movement and those that oppose it (Sabri et al., 2016; Cardona et al., 2020). We can then express mechanical power as a product of the forces and speed of the vehicle. The force inherent in the movement is deduced from the kinetic energy stored in it. The forces that oppose movement are called dissipative forces, which are aerodynamic drag, resistance due to friction with the ground, and resistance force due to the inclination of the road (Singh et al., 2019). Therefore, Equation 1 shows us the mechanical power necessary to move the vehicle.

International Journal of Environmental Sciences
ISSN: 2229-7359
Vol. 11 No. 9s, 2025
https://theaspd.com/index.php

$$p_v = \frac{1}{2}pv(sc_x)v^3 + mgvc_{rr} + mgv\sin(\alpha) + mv\frac{dv}{dt} \quad (1)$$

where is the mass of the vehicle, is the slope of the road, is its speed, is the density of the air, is the frontal area of the vehicle, is the aerodynamic drag coefficient, is gravity, and is the motion resistance coefficient. The parameters are based on a service bus, and are as shown in Table 1, being obtained from $mavpsC_xgC_{rr}$Carignano et al., (2019).

Table 1. Vehicle Parameters

Name	Symbol	Value	Unit
Air density	p	1.2	Kg/m3
Coefficient of resistance to movement	C_{rro}	0.008	S/u
Coefficient of resistance to movement	C_{rrl}	0.00012	s2/m2
Drag coefficient	C_x	0.65	S/u
Front Area	s	8.06	m2
Total Mass	m	14000	Kg
Gravity	g	9.8	m/s2

The total mass of the vehicle includes the mass of the chassis, the powertrain, the components and the weight of the passengers. It should be noted that as the weight of the vehicle increases with the increase in the weight of its components and the number of occupants, more power is needed to reach the speed profile, because there are higher power peaks. Figure 1 shows the powertrain components that will be part of the vehicle's energy management. The main source of unidirectional power is the fuel cell, which is connected to a DC converter. Storage elements (batteries and supercapacitor) are considered bidirectional, as they can deliver energy to movement while also storing energy recovered from braking. These elements are also associated with a DC converter. The speed profile can be placed as a power profile, and must be met by the sources. So, the power balance can be expressed as formulated in Equation 2:

$$p_v = p_{sup} + p_{bat} + p_{fc} + p_{break} \quad (2)$$

where is the power of the supercapacitor, is the power of the battery, is the power of the fuel cell, and is the power dissipated in the mechanical brake. As expressed in Equation 2, the sum of the powers of the elements must be equal to the mechanical power.$p_{sup}p_{bat}p_{fc}p_{break}$

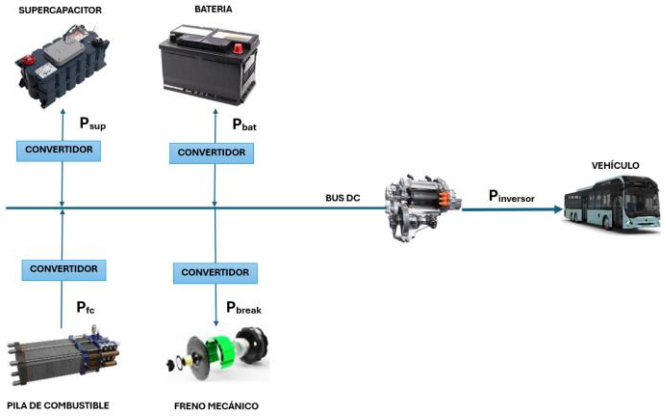

Figure 1. Vehicle architecture

2.3 Battery Model

The essential component of EVHs is the electrochemical battery. For specific energy management, batteries will be described primarily in terms of power and energy. They are distinguished by their rated capacities, as well as the state of charge (SOC), which is a percentage of their maximum capacity that describes the idle energy stored in the battery. Some desirable attributes of batteries for EV and EV applications are high energy density and long cycle life (Feroldi & Carignano, 2016; Carignano et al., 2019).Energy density refers to the total amount of energy a battery can store for a

International Journal of Environmental Sciences
ISSN: 2229-7359
Vol. 11 No. 10s, 2025
https://theaspd.com/index.php

given mass. These cells can store considerable amounts of energy. Other features include long cycle life, low initial and replacement costs, high reliability, wide operating temperature range, and ruggedness. Generally, battery performance is set by a specific SOC window, the constraints of which are the minimum SOC during discharge and the maximum SOC during charging. Internal resistance is the element that restricts the effectiveness of charging and discharging the battery. Under loading and unloading conditions, resistance varies. The non-linear functions of the battery SOC are resistance and open-circuit voltage. A battery model can be extracted from an equivalent circuit, in which the battery is perceived as an open-circuit series voltage source with an internal resistance, as illustrated in Figure 2.

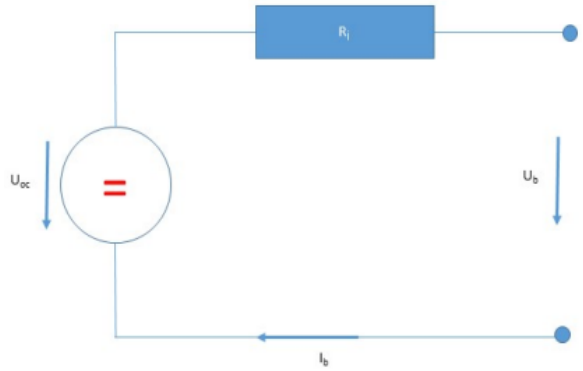

Figure 2. Equivalent battery circuitry.

Depending on the amount of voltage/current, we connect a set of batteries, in series, in parallel or a mixed series-parallel connection. For a series connection, the voltage supplied by the assembly is equal to the sum of the voltages. In parallel, the current increases with the sum of the number of batteries inserted. In both cases, the capacity always increases. According to Carignano et al., (2019), the equations for charging and discharging battery energy should be considered as a function of the SOC, where is the charging power and is the discharging power, as described in Equations 3 and 4, respectively.$p_{cb}p_{db}$

$$p_{cb}(k) = -\frac{n_{bats}u_{cmax}^2 - u_{oc}(k)u_{cmax}}{r_i}\, n_{batp} \quad (3)$$

$$p_{db}(k) = \frac{-n_{bats}u_b(k)^2 + u_{oc}(k)u_{cmin}}{r_i}\, n_{batp} \quad (4)$$

where is the battery voltage, is the open circuit voltage of the battery, is the internal resistance of the battery, where is the number of cells in parallel and is the number of cells in series and is the discrete time. The open-circuit voltage of supercapacitors is a function of the battery charge. The total power of the battery will be the sum of y , and is called . The battery is also associated with a dbat converter efficiency, which takes into account losses in the converters and takes a value of 0.98. We can then define the total power of the pbat battery as shown in Equation 5.$u_b u_{oc} r_i n_{batp} n_{bats} k p_{db} p_{cb} p_{bat}^*$

$$p_{bat}(k) = \delta_{bat}\, p_{bat}^*(k) \quad (5)$$

On the other hand, the battery under consideration is a prismatic Ni-MH battery in a resin housing, where its parameters are shown in Table 2 and have been taken from Prabhakar & Ferdowsi, (2008).

Table 2. Battery parameters

Parameter	Information
Maker	PEVE
Form	Prismatic
Cover	Plastic
Cell Capacity (Ah)	6.5
Cell Voltage (V)	7.2

Specific energy (Wh/kg)	46
Specific Power (W/kg)	130
Mass (kg)	1.04
Operating Temperature (°C)	-20 to 50
Cost (€/kg)	33.88

2.4 Supercapacitor Model

Supercapacitors are energy accumulators. The specific power, or instantaneous power, they can deliver is greater than that of batteries, but their specific energy, or the amount of energy they can store, is substantially less (W. Zhou et al., 2023). In certain situations, supercapacitors are employed as Energy Storage Systems (ESS), while in other situations, such as in this article, they can be located as a secondary storage system. This allows for better performance of both the primary power system and the ESS. The equivalent circuit of the supercapacitor consists of a capacitor representing capacitance and a series resistor representing ohmic losses in the electrodes and electrolyte (Parvini et al., 2016). In the model, we will redefine the equations as a function of the capacitor's Energy State (SOE). A detailed study of the process can be found at Feroldi & Carignano, (2016). So, Equation 6 shows how SOE is defined.

$$SOE(k) = \frac{e_{sc}(k)}{e_{sc,t}} \quad (6)$$

where is the total storable energy and is the instantaneous energy. So, it is defined as a sample in Equation 7:$e_{sc,t} e_{sc} e_{sc}$

$$e_{sc}(k) = \frac{1}{2} c_{sc} q_{sc}^2(k) \quad (7)$$

where is the capacitor voltage expressed in (V), and is the capacitance expressed in (F). $q_{sc} c_{sc}$

For Feroldi & Carignano, (2016), the charging power and the discharging power are given by Equation 8 and 9, respectively:$p_{cs} p_{ds}$

$$p_{cs}(k) = \frac{n_{sc} u_{sc,max} (u_{sc}(k) - u_{sc,max})}{r_{sc}} \quad (8)$$

$$p_{ds}(k) = \frac{n_{sc} u_{sc,min} (u_{sc}(k) - u_{sc,min})}{r_{sc}} \quad (9)$$

where is the number of elements, and is the voltage limits of the supercapacitor, is the open-circuit voltage, and is the resistance of the circuit. In $n_{sc} u_{sc,max} u_{sc,min} u_{sc} r_{sc}$Feroldi & Carignano, (2016) we can find a more detailed analysis and parameters. The parameters used are from the Maxwell 125V heavy transport module and are shown in Table 3.

Table 3. Supercapacitor Parameters

Parameter	**Information**
Maker	PEVE
Packing	Bulk
Cell capacitance (F)	3000
Nominal voltage (V)	125
Temperature (°C)	-45 to 65
Mass (kg)	1.3
Specific Power (W/kg)	1700
Specific energy (Wh/kg)	2.3
SOEmax	1
SOEmin	0
Cost (€/kg)	88.34

International Journal of Environmental Sciences
ISSN: 2229-7359
Vol. 11 No. 10s, 2025
https://theaspd.com/index.php

The power of the supercapacitor is the sum of y . The supercapacitor system is associated with a converter efficiency shown in Figure 1, which represents losses in the converters. In the current job, this parameter will take a value of 0.95. Then, the total power output of the supercapacitor system is given by Equation 10:$p_{sup}p_{cs}p_{ds}\delta_{sup}p_{sup}$

$$p_{sup}(k) = \delta_{sup}\, p_{sup}(k)^* \qquad (10)$$

2.5 Fuel cell model

PEMFC fuel cells have two electrodes: the anode, where the fuel is oxidized, and the cathode, where the oxidizer is reduced (Carignano et al., 2019; Hoogers, 2002). The electrolyte simultaneously acts as an electrical insulator and a proton conductor. In addition, it distinguishes reactions in the anodes and cathode. The electrons move from the anode to the cathode through an external circuit that produces electric current, while the protons travel through the electrolyte. Inside the cathode, electrons, protons, and oxidants are decreased, producing byproducts. In this type of fuel cell, hydrogen is often used as an oxidizing agent and oxygen as a reducing agent. The voltage variation produced by a single mono unit or cell is less than one volt, which is why it is necessary to connect multiple mono cells in series to achieve the appropriate voltage for the necessary use. However, although the fuel cell is the main component of a fuel cell system, the complete system usually includes the following subsystems: Fuel Supply, Oxidizer Supply, Water Management, Heat Management, Instrumentation, and Power Conditioning Controls.The fuel and oxygen inlet lines to each cell are connected in parallel to achieve similar pressure at the anode and cathode. Impedance is a function of fuel pressure, membrane moisture, and catalyst state. To characterize the model to be used, it is understood that power is the product of current and potential. Power density is the product of potential and current density, so it can be represented as described in Equation 11.

$$p_{fc} = v_{fc}i_{fc} \qquad (11)$$

Generally, the power density is represented in relation to the current density by means of the so-called polarization curves, which indicate that there is a maximum power density that a fuel cell can have. Fuel cells cannot always be operated at their maximum power levels. Figure 3 shows the polarization curve and the power-current curve used in this study for the fuel cell.

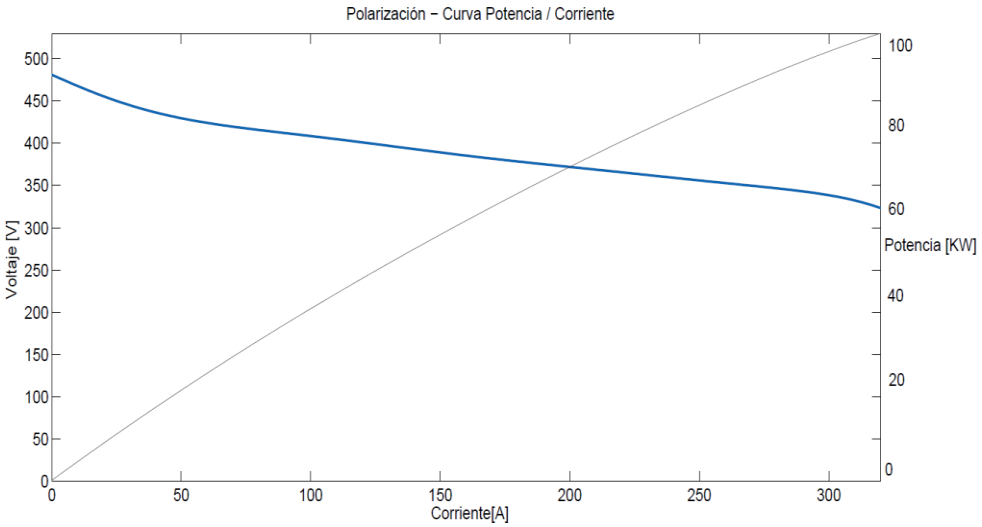

Figure 3. Polarization and power-current curve of the fuel cell.

In this study, we have obtained the fuel cell curve for a fuel cell system with BALLARD XD6 FCvelocity module. This curve has been sized according to the maximum power of the driving profiles to be used, which are detailed in the next section. Thus, there is a maximum power that the cell can achieve, since the efficiency of the fuel cell is directly related to the potential of the fuel cell. Equation 12 shows us the efficiency of a fuel cell.

$$n_{fc} = \frac{p_{fc}}{p_{H_2}} \quad (12)$$

where is the electrical power produced and is the theoretical power associated with the hydrogen consumed, which is defined as indicated in Equation 13.$p_{fc} p_{H_2}$

$$p_{H_2} = \frac{p_{fc} + p_{com}}{\eta_{therm} \cdot \eta_{util} \cdot \eta_{fci}} \quad (13)$$

where is the power demanded by the compressor, is the thermodynamic efficiency (0.98 to 298 K), is the efficiency of use of the cell, defined as a ratio between the mass of fuel that reacted and the mass that entered the fuel cell; and is the efficiency of each cell, calculated as the ratio of the cell voltage to the open-circuit voltage. This relationship can also be expressed as a function of the voltage and current of the cell, as shown in Equation 14.$p_{com} \eta_{therm} \cdot \eta_{util} \eta_{fci} v_{fc} E_{oc}$

$$n_{fc} = \frac{v}{1.482} \cdot \frac{i}{(i + i_{loss})} \quad (14)$$

The losses, called , are typically small. Superior efficiency can be achieved with the same fuel cell, while maintaining a noticeably lower power density level. This means that, for a required power, a fuel cell can be expanded (with a larger active area) and made more efficient ii_{loss}(Barbir, 2005).

Equation 15 allows us to obtain an electrical model that characterizes the fuel cell using voltage and current equations.

$$u_{fc} = E_{oc} - u_{act} - u_{ohmic} \quad (15)$$

u_{fc} is the output voltage of the system, the ohmic loss voltage is and the activation voltage drop as . Whereas, it is the open circuit of voltage defined by Equation 16.$u_{ohmic} u_{act} E_{oc}$

$$E_{oc} = k_c \left[E_o + \left(T_{fc} - T_{ref} \right) \frac{-\alpha_{T_{ref}}}{zF} + \frac{RT}{zF} ln \left(P_{H_2} P_{O_2}^{1/2} \right) \right] \quad (16)$$

where f is a temperature constant, is the electromotive force under standard pressure conditions, is the reference temperature, is the nominal voltage constant, is the operating temperature, is the electron transfer number, which can be obtained as shown in $\alpha_{T_{ref}} E_o T_{ref} k_c T_{fc} z$(Zhou et al., 2016). Whereas, , are the pressure of the gas, it is the Faraday constant and it is the constant of the gas. The activation voltage drop, , is given by Equation 17.$P_{H_2} P_{O_2} F R u_{act}$

$$u_{act} = \frac{1}{\tau s + 1} N A_{nom} ln \left(\frac{i_{fc}}{i_o} \right) \quad (17)$$

where is the voltage time constant and is the number of cells. Equation 18 tells us the ohmic voltage drop, .$\tau N u_{ohmic}$

$$u_{ohmic} = r_{internal} i_{fc} \quad (18)$$

Where the output current of the cell is and the internal resistance of the fuel cell system is . The parameters of the fuel cell assembly are shown in Table 4. $i_{fc} r_{internal}$

Table 4. HD 100 FCvelocity Ballard Fuel Cell Parameters.

Parameter	Information
Maximum Voltage	580 V
Maximum Current	288 A
Number of cells	560

Operating Temperature	330 °K
Nominal air pressure	2.24
Maximum power	1oo kW
Mass	285 kg
Reference temperature	298 °K
Constant temperature	44.43
Cost	100 k€

Finally, hydrogen consumption is defined according to Equation 19.

$$m_{H_2} = \frac{NM_{H_2} i\lambda}{nF} \quad (19)$$

Where the mass of hydrogen consumed is , the molar mass of hydrogen as , the ratio of excess hydrogen is , while the number of electrons acting in the reaction is defined as .$m_{H_2} M_{H_2} \lambda n$

2.6 Speed profiles

A driving cycle consists of a speed profile that defines the route that the vehicle must follow. Some types of vehicles follow specific cycles, such as urban transport, which follows predefined urban routes. Different driving cycles have been created that more accurately represent the driving conditions of the vehicles (Tzirakis et al., 2013). For example, the European ECE15 cycle, whose main drawback is smooth accelerations; the USFTP 72 cycle, which symbolizes driving conditions in Los Angeles; and the USFTP 75 cycle, used for emissions certification in the United States.
However, in this paper we will present two specific driving cycles, the Buenos Aires Transport Driving Cycle (BADC), and the Manhattan Driving Cycle (Manhattan DC), as they are driving cycles designed for city buses, such as those indicated in Table 1, which consider the driving conditions of these buses, which have several stops and decelerations. which allows a significant amount of energy to be recovered.

2.7 Driving Cycle of the City of Buenos Aires

For the elaboration of the Buenos Aires Driving Cycle (BADC), 30 h of GPS information were obtained, corresponding to 51 bus trips that covered a total of 313.6 km. The BADC was validated in a reference diesel bus widely used in Buenos Aires and the fuel consumption results obtained were compared with those reported by the bus line operator. Figure 4 shows the speed profile and Table 5 presents more salient characteristics.

Table 5. BADC driving cycle parameters.

Parameter	**Value**
Total cycle time	1864 s
Average speed	3.92 m/s
Maximum speed	15.6 m/s
Maximum acceleration	9.2155x10-5 m/s2
e_v^+	22678.62 kJ
e_v^-	11870.63 kJ

Using Equation 1, we can obtain the instantaneous power needed to follow this profile. The equation allows us to obtain the power values, , which are the instantaneous values that need to be delivered to produce motion. The sum of these power values, for the complete profile, becomes the energy needed to produce motion, . We can also obtain the power values that we can recover through regenerative braking, . Similarly, the sum total of $p_v^+ e_v^+ p_v^-$

International Journal of Environmental Sciences
ISSN: 2229-7359
Vol. 11 No. 9s, 2025
https://theaspd.com/index.php

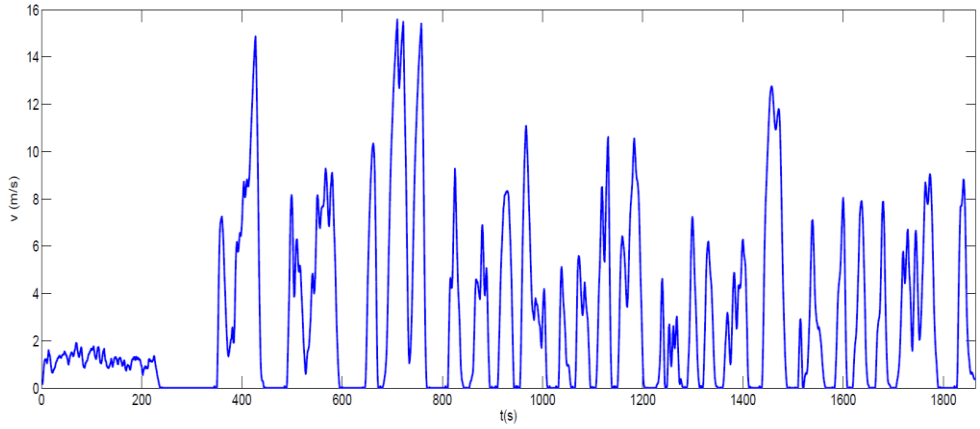

Figure 4. BADC Driving Cycle

These power values, for the complete profile, will be the energy recovered when braking. Similarly, the equation allows us to get the maximum instantaneous power that needs to be delivered, and the maximum instantaneous power that can be recovered when braking, which is useful for sizing storage systems.$e_v^- p_{maxv}^+ p_{minv}^-$
Using the ratio given in Equation (19), we can obtain the maximum amount of energy that can be recovered when there are no losses. For the BADC, this amount is 52.34%.

$$\%recovery = \frac{e_v^-}{e_v^+} \quad (20)$$

2.8 Manhattan Driving Cycle
This driving cycle used for bus testing in New York has a distance traveled of 3.30 km, with a driving time of 1089 s and a maximum acceleration of 2.04 m/s2. Figure 5 shows the speed cycle of the Manhattan skyline. Table 6 shows the most relevant parameters of the profile. In the same way as for the BADC profile, and using Equation 20, the maximum amount of energy that can be recovered from braking for this profile is 58.84%.

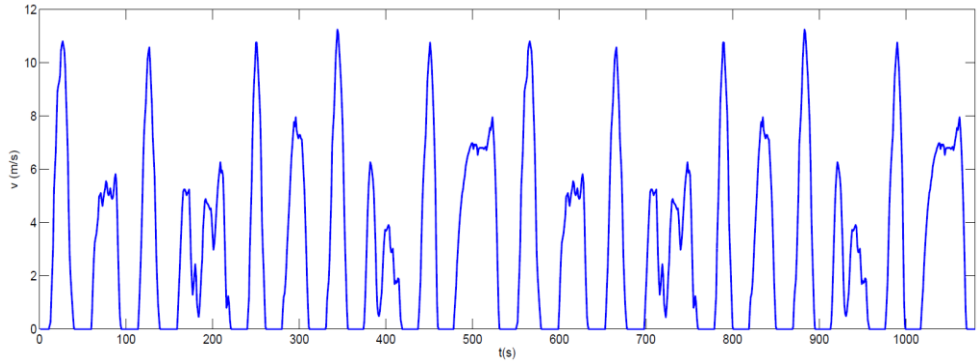

Figure 5. Manhattan Driving Cycle

Table 6. Manhattan driving cycle parameters.

Parameter	Value
Total cycle time	1089 s
Average speed	3,033 m/s
Maximum speed	11.24 m/s
Maximum acceleration	2,044 m/s2
e_v^+	13747.04 kJ
e_v^-	8090.08 kJ

2.9 Model-Oriented Economic Predictive Control (EMPC)

Usually, traditional predictive control aims to penalize deviations in future control actions in relation to the reference trajectory established according to the needs of the process to be implemented. In the case of EMPC control, when applied to energy management systems, the cost function takes the form shown in Equation 21.

$$J = min\left(\sum_{K=0}^{Hp-1} f_1(k) + \sum_{K=0}^{Hp-1} f_2(k) + \sum_{K=0}^{Hp-1} f_3(k)\right) \quad (21)$$

The function can be defined as the economic cost of the operation, and can be formulated as shown in Equation 22. On the other hand, it is responsible for establishing the safety limits in energy storage devices, which is of vital importance to preserve the useful life of the elements. $f_1 f_2$

In order to analyze the wear of the elements in the operation, it is necessary to study the models of health states (SOH), in this case for the battery and the supercapacitor. These are summarized by Equation 23. Finally, it is the one that specifies the smooth operation of the control actions, which is aimed at limiting and avoiding sudden peaks in the main generation element, which is the fuel cell. It can also avoid these abrupt variations in storage elements and is expressed by Equation 24. f_3

$$f_1(k) = w_\infty u(k)\Delta(t) \quad (22)$$

$$f_2(k) = \in (k)^T w_x \in (k) \quad (23)$$

$$f_3(k) = \Delta u(k)^T w_u \Delta u(k) \quad (24)$$

In these equations, it is related to the weight of the economic cost function on , while it is the penalty value of the constraints that are related to the safety values applied to the SOCs of the storage elements. it is the matrix of weights that is associated with these penalties. It is also defined as the vector of variations in the control signal and as the matrix of weights that is associated with the control actions. The variation in the weight of the control actions will allow us to restrict the operation of the system towards $w_\infty J \in (k) w_x \Delta u(k) w_u f_1, f_2$, and , that is, towards preserving the useful life of the elements, towards strengthening the peaks or the smooth operation of them. f_3

2.10 Control-oriented model

This section describes the model proposed for the controller, which considers all the components of the VEH in relation to the power distribution described to achieve the movement of the vehicle overcoming all the forces contrary to it, and also takes into account its operational restrictions. The models proposed in this work consider the upper layers of the control stages, that is, where the energy contribution of the elements to the vehicle is determined to facilitate its movement. Energy and power models are useful to be able to orient and solve the problems of load flow towards lower elements that allow the transformation of voltages and currents, towards the operating values.

This means that the control model needs to improve the flow in the power bus represented in Figure 1. Equation 25 describes the behavior of the battery, Equation 26 that of the supercapacitor, and Equation 27 that of the fuel cell. In the first two, the energy is defined in relation to the SOC to correspond to the models analyzed, while in the third in terms of the same variable.

$$SOC_{bat}(t) = SOC_{bat,0} + \int_0^t \frac{p_{bat}(t)dt}{e_{maxbat}} \quad (25)$$

$$SOE_{sup}(t) = SOE_{sup,0} + \int_0^t \frac{p_{sup}(t)dt}{e_{maxsup}} \quad (26)$$

$$e_{fc}(t) = e_{fc,0} + \int_0^t p_{fc}(t)dt \quad (27)$$

International Journal of Environmental Sciences
ISSN: 2229-7359
Vol. 11 No. 9s, 2025
https://theaspd.com/index.php

Equations 25, 26 and 27 are placed in a space of states described in Equations 28 and 29, to be entered into the cost function.

$$x(k+1) = Ax(k) + B_u(k) + B_p(k) \quad (28)$$

$$E_u(k) + E_d d(k) = 0 \quad (29)$$

$x(k) \in^n$ it is the vector of states, it is the vector of control variables, it represents the power demand that is given by the speed profiles; A, B, and B are the state matrices, while, and describe the equilibrium relationship for the power bus.$u(k) \in^m d(k) \in^p EE_d$
Control techniques can use the space of states, which will be reduced by Equation 21. It is important to note that the storage components would be sized with 20% of the total value of the maximum power of the fuel cell, and their weight is included in the weight of the service bus. The limitations are set out in Equations 30, 31, 32, 33 and 34.

$$0 \leq p_{fc} \leq p_{fcmax} \quad (30)$$

$$p_{batmin} \leq p_{bat} \leq p_{batmax} \quad (31)$$

$$p_{supmin} \leq p_{sup} \leq p_{supmax} \quad (32)$$

$$SOE_{min} \leq SOE \leq SOE_{max} \quad (33)$$

$$SOC_{min} \leq SOC \leq SOC_{max} \quad (34)$$

So, the maximum power of the battery is equal to 10 kW, the minimum power of the battery is equal to -10 kW, the maximum power of the supercapacitor is equal to 20 kW, the minimum power of the supercapacitor is equal to -20 kW. The SOC values for the battery and supercapacitors are: 0.1, 1, 0.3, and 0.9. $p_{batmax} p_{batmin} p_{supmax} p_{supmin} SOE_{min} SOE_{max} SOC_{min} SOC_{max}$

3. DISCUSSION OF THE RESULTS

In the first instance, as mentioned in previous sections, we need to know the power resulting from the driving cycles.

3.1. Buenos Aires Driving Profile (BADC)

When applying equation 1, with the speed values of the BADC cycle and the parameters of Table 1 referring to the characteristics of the bus, the total energy needed to generate the profile is 22,656,824.54 J. Figure 6 shows the power profile for BADC.

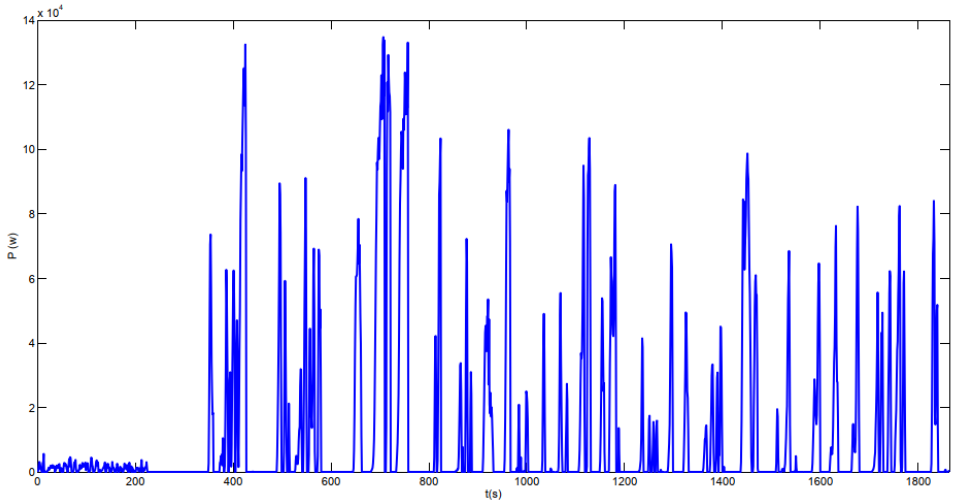

Figure 6. Power developed by the BADC driving profile

International Journal of Environmental Sciences
ISSN: 2229-7359
Vol. 11 No. 10s, 2025
https://theaspd.com/index.php

3.2. Manhattan Driving Profile

The value of energy required to meet the velocity profile is 13,733,703.09 J, while the maximum recoverable energy is 8,081,852.64 J. Figure 7 shows the power profile generated by the application of Equation 1 with the parameters in Table 1 and the speed of the profile to be worked.

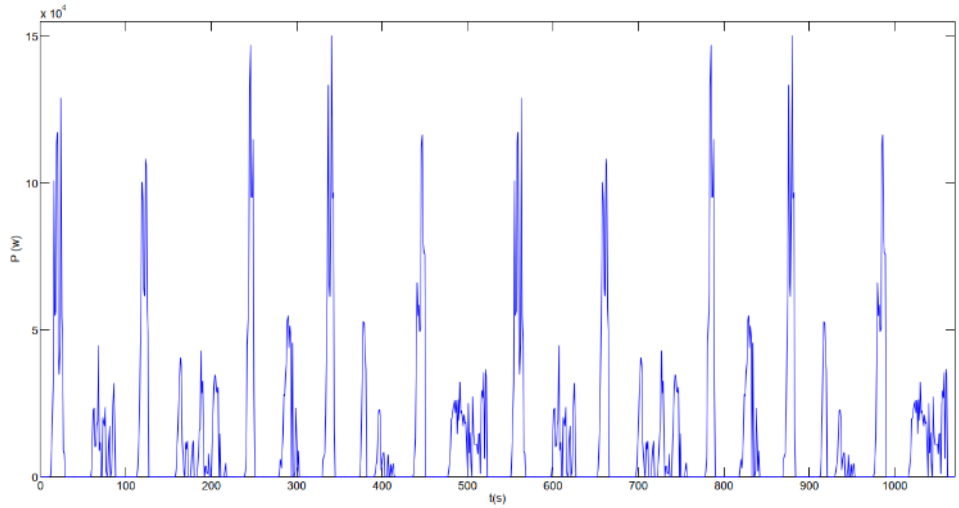

Figure 7. Power developed by the Manhattan Driving Profile

3.3. Compliance with power profiles with the EMPC controller.

Equation 21, which has been called the cost function, is made up of 3 terms that are visualized in Equations 22, 23 and 24, respectively. In each of these last mentioned equations there is a weight, which can range between 0 and 1. That is, it can take different values simultaneously. In the case of this article, the weights have been varied from 0.1 to 0.1 and a comparative graph has been made of the relationship between the weights and the decrease and increase of the restriction for each of the 3 functions $wf_{1,}, f_2$and f_3.

Figure 8 shows the relationship between two functions for the BADC profile, the same as the economic function compared to the security function $f_1 f_2$. As expected, while the weight of one function increases, that of the other function decreases, and thus shows how while the economic function decreases, the importance of maintaining safety thresholds increases.

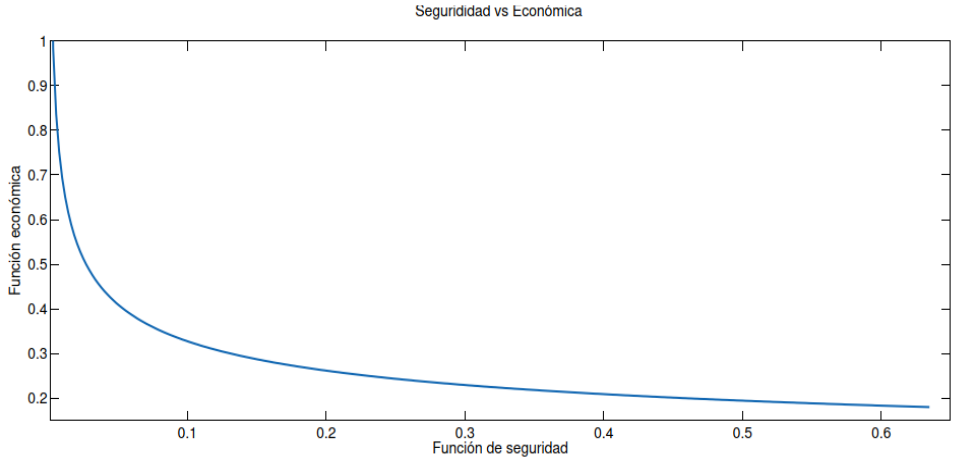

Figure 8. Relationship between and of the total cost function$f_1 f_2$

Figure 9 shows the relationship between the economic functions and the control function. In the same way as in the previous case, while one decreases, the other increases. With both graphs made for the BADC profile, we want to show that the values of the weights can be any between 0 and 1, and that depending on this particular we will have more or less action of a function within the total cost function.$f_1 f_2$

International Journal of Environmental Sciences
ISSN: 2229-7359
Vol. 11 No. 9s, 2025
https://theaspd.com/index.php

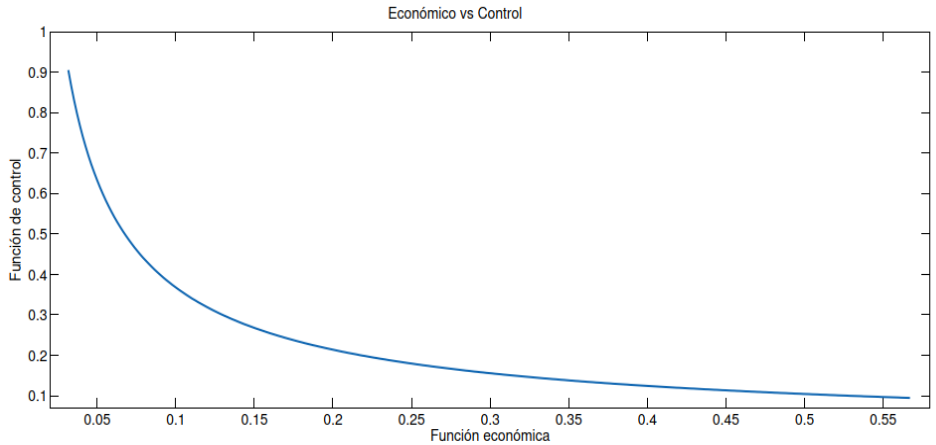

Figure 9. Relationship between and of the total cost function $f_1 f_3$

Then, as a future contribution, a Pareto study can be done to determine the best weighings. For the study in particular, we have taken weights of 0.33 for each of the vectors w, so that we weigh all the components of the proposed cost function in the same way. For the case of the BADC profile, Figure 10 shows the balance of power delivered by the fuel cell, battery and supercapacitor to meet the BADC speed profile. Table 7 shows the percentage contribution of each source to obtain the energy required for movement.

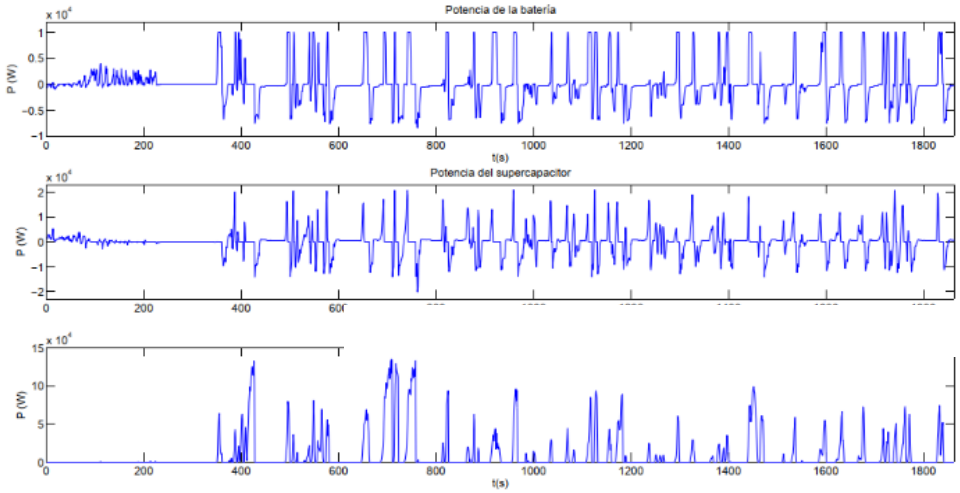

Figure 10. Power balance by source for the BADC profile

Table 7. Energy delivered by each source for the BADC profile

Element	Power Delivered	Percentage
Fuel Cell	J 18,530,700.82.	81.71 %
Batteries	1,669,146.46 J.	7.36 %
Supercapacitor	2,481,041.08 J.	10,94 %

To verify that the compliance or performance of the controller is adequate, the sum of the powers of the elements that are part of the scheme in Figure 1, including dissipation, has been compared with the power of the profile, resulting in Figure 11.

International Journal of Environmental Sciences
ISSN: 2229-7359
Vol. 11 No. 10s, 2025
https://theaspd.com/index.php

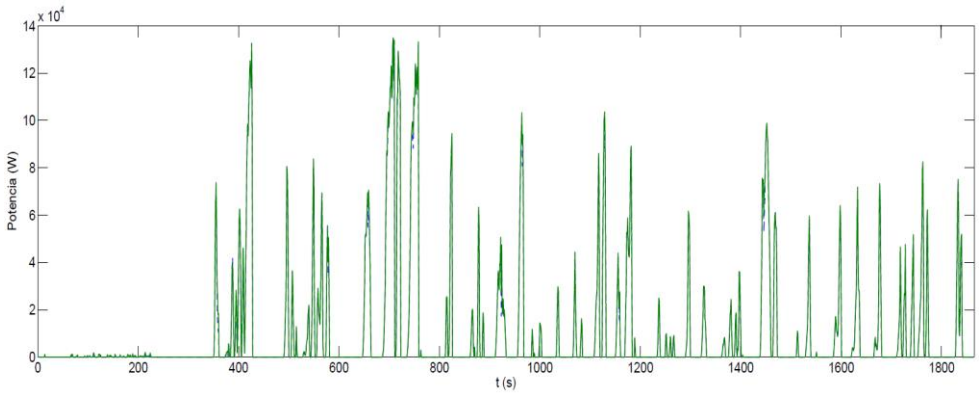

Figure 11. BADC Power Profile Compliance

In the case of the Manhattan driving profile, Table 8 shows the percentage contribution of the elements of the generation train that is composed of the sources of the system, called fuel cells, batteries and supercapacitors. Figure 12 graphically shows the contribution over time of the driving profile of the named sources.

Table 8. Power delivered by each source for the Manhattan skyline

Element	Power Delivered	Percentage
Fuel Cell	J 10,944,020.93.	79.61 %
Batteries	1,277,100.29 J.	9.29 %
Supercapacitor	J1,525,927.77.	11.10 %

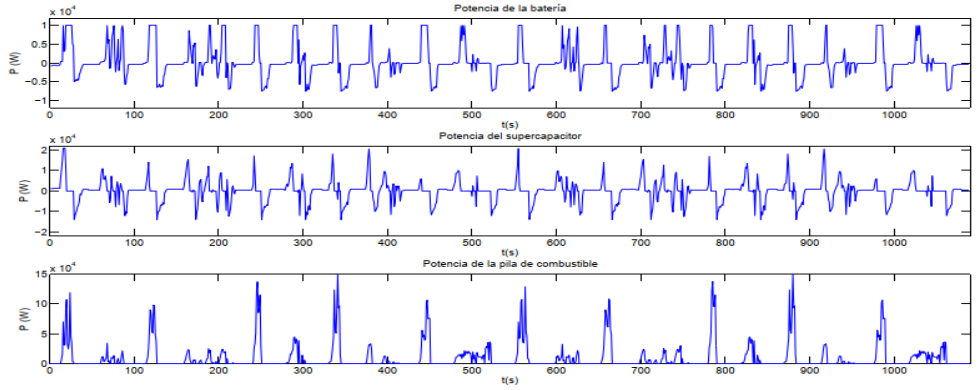

Figure 12. Power Balance by Source for the Manhattan Profile

Finally, Figure 13 shows that the power profile is met, with the comparison of the power input given by the controller versus the power demanded for the fulfillment of the Manhattan profile.

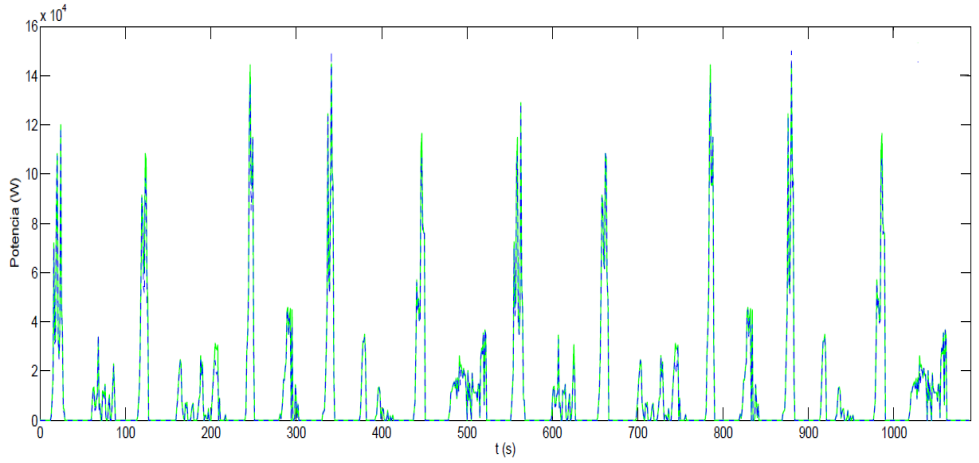

Figure 13. Manhattan Power Profile Compliance

3.4. Study of the contributions by varying the prediction horizon of the controller.

For the present, a prediction horizon of 60 seconds, i.e. 1 minute, has been considered within the controller's parameters. The closer this value is to the final time of the driving profile, the more information about the speed values is given to the controller at future times. However, the longer the prediction horizon, the higher the computational cost and therefore it is far from reality. This would imply an unrealistic driving scenario. Considering that response times would be slow and this is not convenient in vehicle automations. Tables 9 and 10 show the contributions of the 3 elements considered in the system, as the prediction horizon increases.

Table 9. Power delivered by the powertrain elements for the Hs variation on the Manhattan skyline

Manhattan Driving Cycle								
Prediction Horizon (Hs)	60	100	300	500	700	900	1000	1089
Fuel Cell (%)	79.61	79.43	79.01	78.71	78.23	77.87	77.61	77.36
Battery (%)	9.29	9.21	9.08	8.96	8.83	8.71	8.67	8.59
Supercapacitores (%)	11.1	11.36	11.91	12.33	12.94	13.42	13.72	14.05

Table 10. Energy delivered by the propulsion system elements for Hs variation in the BADC profile

Driving Cycle Buenos Aires								
Prediction Horizon (Hs)	60	300	500	700	900	1300	1600	1869
Fuel Cell (%)	81.71	80.45	19.89	79.03	78.46	77.03	76.23	75.52
Battery (%)	7.36	7.67	8.03	8.25	8.43	9.01	9.23	9.41
Supercapacitores (%)	10.94	11.88	12.08	12.72	13.11	13.96	14.54	15.07

It will be noted that the use of the fuel cell decreases, to avoid the consumption of hydrogen as the main fuel, and therefore a greater recovery of the sum of energy from the battery and the supercapacitor. This study seeks to demonstrate that the controller responds both to variations in the cost function and to variations in its internal parameters according to the MPC control theory.

4. CONCLUSIONS

The present study has some important contributions, such as the use of two energy storage sources, to be able to adequately distribute the energy generated by the concept of regenerative braking in speed profiles such as the BADC and the Manhattan, where there are important moments of deceleration. For example, the total recovery with the BADC driving profile, when the base equation of the power model is applied to equation 1, is about 52%. However, these values are not achievable by the size or capacity of the storage elements, because the more of them you have, the more mass and cost of the elements increases. However, in the review of the literature cited in this article, it can be observed that, for ideal control cases, with the use of techniques such as dynamic programming, among others, which have an infinite prediction horizon, for similar capacities of storage elements the recovery is about 19 to 20%. The present work, with the configuration of equivalent weights for the three control functions within the cost function, achieves a recovery of close to 18%. This implies that the controller's approach and constraints meet their objective. In the same way, both the BADC profile and the Manhattan profile are able to meet the energy balance requested by the demand, thus meeting the proposed speed profile. The cost function has the advantage that operating costs can be involved within it, penalizing the operation outside the efficiency zones, and also the useful life of the elements by approximating within the space of states, models of the health of the components. The relationship between the weighing of the functions of the cost functional has been raised in the same way, which allows us to determine that there is a relationship between them that contributes to the control criteria. Future work may be the implementation of a Pareto chart, to establish the optimal weights for the needs to be solved in terms of efficiency, useful life and

operation of the main sources and storage. The study of the prediction horizon allows us to verify that when it increases, we approach an optimal control with recovery similar to that of the literature, however, it is not a realistic scenario for driving, which implies an increase in computational time and cost. Finally, it should be noted that a decrease in the contribution of the fuel cell of about 20% is achieved, reducing its maximum peaks and the instants of start-up time, so that the operation in regions of efficiency of the components is achieved, providing lower hydrogen consumption and a longer useful life of the components by sizing a SOC and SOE window.

REFERENCES

Alvarez Díaz, L. J. (2023). Electric vehicles: Analysis of their evolution and their impact on the Paraguayan economy. Period 2018 – 2022. *Regional Development (Encarnación)*, *1*(2), 74-80.

Barbir, F. (2005). *PEM Fuel Cells: Theory and Pactice* (Segunda). Academic Press. https://doi.org/10.1016/B978-0-12-078142-3.X5000-9

Barceló Serra, R. de P. (2023). *Evolution of the electricity demand associated with the deployment of electric vehicles on the island of Mallorca, for the year 2030*. http://dspace.uib.es/xmlui/handle/11201/167216

Bedoya Caro, I. D., Amell Arrieta, A., Cadavid, F. J., & Pareja, J. A. (2007). Effect of the degree of load and the amount of pilot fuel on the environmental mechanical behavior of a dual diesel-biogas engine for electricity generation. *Revista Facultad de Ingeniería Universidad de Antioquia*, *42*, 79-93. Redalyc.

Bragagnolo, S. N., Vaschetti, J. C., Magnago, F., Gomez-Targarona, J. C., Bragagnolo, S. N., Vaschetti, J. C., Magnago, F., & Gomez-Targarona, J. C. (2020). Demand management in smart grids. Perspective and control from the user and the distributor. *Information technology*, *31*(3), 159-170. https://doi.org/10.4067/S0718-07642020000300159

Cardona, A., Jaramillo Álvarez, J. S., & Amell Arrieta, A. A. (2020). Evaluation of the mechanical and environmental performance of a diesel engine ignition mode caused by biogas enriched with CH4 and hydrogen. *Scientia et Technica*, *25*(1), 65-76.

Carignano, M., Roda, V., Costa-Castelló, R., Valiño, L., Lozano, A., & Barreras, F. (2019). Assessment of Energy Management in a Fuel Cell/Battery Hybrid Vehicle. *IEEE Access*, *7*, 16110-16122. https://doi.org/10.1109/ACCESS.2018.2889738

Feroldi, D., & Carignano, M. (2016). Sizing for fuel cell/supercapacitor hybrid vehicles based on stochastic driving cycles. *Applied Energy*, *183*, 645-658. https://doi.org/10.1016/j.apenergy.2016.09.008

Gadvay Lara, C. J., & Monar Argüello, C. M. (2021). *Use of automotive software to reduce polluting emissions from an electronically injected vehicle by modifying flash memory without affecting its torque and power in the city of Riobamba*. http://dspace.espoch.edu.ec/handle/123456789/15396

García, G. G.-E. (2024). The transition to electric vehicles: Evolution and problems. *ICE Economic Bulletin*, *3172*, Article 3172. https://doi.org/10.32796/bice.2024.3172.7813

Solar Energy Management and Sustainability. (2023). *Educational Format*. https://www.formatoedu.com/masters/gestion-de-la-energia-solar-y-sostenibilidad/

Guzzella, L., & Onder, C. H. (2010). *Introduction to Modeling and Control of Internal Combustion Engine Systems*. Springer. https://doi.org/10.1007/978-3-642-10775-7

Hoogers, G. (2002). Fuel cell technology handbook. En *Fuel Cell Technology Handbook* (p. 345).

Lozano, I. F. S. (2024). Evaluation of torque, power and fuel consumption with the implementation of a hydrogen cell in a 1.6 lt gasoline vehicle. *Polo del Conocimiento*, *9*(7), 3112-3127. *https://doi.org/10.23857/pc.v9i8.7782*

Martínez Pérez, F., & Gassinski, L. (2022). Energy efficiency and the role of maintenance in it. *Energy Engineering*, *43*, 10-18.

Melo Espinosa, E. A., Sánchez Borroto, Y., Ferrer Frontela, N., & Ferrer Frontela, N. (2012). Evaluation of a spark-ignition engine working with ethanol-gasoline mixtures. *Energy Engineering*, *33*(2), 94-102.

Méndez Cruz, O. (2024). Analysis of the cost of mitigating carbon emissions attributable to the integrated participation of solar, wind and biomass generation in the national interconnected electricity system, during 2021. *Pedro Ruiz Gallo National University*. http://repositorio.unprg.edu.pe/handle/20.500.12893/12947

Mittal, V., & Shah, R. (2024). Energy Management Strategies for Hybrid Electric Vehicles: A Technology Roadmap. *World Electric Vehicle Journal*, *15*(9), Article 9. https://doi.org/10.3390/wevj15090424

Mohamed Khaleel, Nassar, Y., J. El-Khozondar, H., Monaem Elmnifi, Rajab, Z., Yaghoubi, E., & Yaghoubi, E. (2024). Electric Vehicles in China, Europe, and the United States: Current Trend and Market Comparison. *Int. J. Electr. Eng. and Sustain.*, *2*(1), 1-20.

Monterroza-Ríos, Á. D., Escobar-Gómez, V. A., Monterroza-Ríos, Á. D., & Escobar-Gómez, V. A. (2021). Technological education in Colombia. An epistemic framework for rethinking a conceptual problem. *Science Technology Society Trilogy*, *13*(25). https://doi.org/10.22430/21457778.1759

Parvini, Y., Siegel, J. B., Stefanopoulou, A. G., & Vahidi, A. (2016). Supercapacitor Electrical and Thermal Modeling, Identification, and Validation for a Wide Range of Temperature and Power Applications. *IEEE Transactions on Industrial Electronics*, *63*(3), 1574-1585. https://doi.org/10.1109/TIE.2015.2494868

Prabhakar, A. J., & Ferdowsi, M. (2008). Comparison of NiMH and Li-ion batteries in automotive applications. *Proceedings of the IEEE Vehicle Power and Propulsion Conference*, 1-6. https://doi.org/10.1109/VPPC.2008.4677500

Rodríguez Tapia, S. E., & Plasencia Caiza, W. G. (2021). *Adaptation of an internal combustion engine to a carburetor to an injection system and verification of torque and power on a dynamometer*. http://dspace.espoch.edu.ec/handle/123456789/16004

Sabri, M. F., Danapalasingam, K. A., & Rahmat, M. F. (2016). A review on hybrid electric vehicles architecture and energy management strategies. *Renewable and Sustainable Energy Reviews*, *53*, 1433-1442. https://doi.org/10.1016/j.rser.2015.09.036

Sinézio Martins, E., Lépine, J., & Corbett, J. (2024). Assessing the effectiveness of financial incentives on electric vehicle adoption in Europe: Multi-period difference-in-difference approach. *Transportation Research Part A: Policy and Practice*, *189*, 104217. https://doi.org/10.1016/j.tra.2024.104217

Singh, K. V., Bansal, H. O., & Singh, D. (2019). A comprehensive review on hybrid electric vehicles: Architectures and components. *Journal of Modern Transportation*, *27*(2), 77-107. https://doi.org/10.1007/s40534-019-0184-3

Tzirakis, E., Pitsas, K., Zannikos, F., & Stournas, S. (2013). Vehicle emissions and driving cycles: Comparison of the Athens driving cycle (ADC) with ECE-15 and European driving cycle (EDC). *Global NEST Journal*, *8*(3), 282-290. https://doi.org/10.30955/gnj.000376

Ulutas, A., Altas, I. H., Onen, A., & Ustun, T. S. (2020). Neuro-Fuzzy-Based Model Predictive Energy Management for Grid Connected Microgrids. *Electronics*, *9*(6). https://doi.org/10.3390/electronics9060900

Zhou, R., Zheng, Y., Jaroniec, M., & Qiao, S.-Z. (2016). Determination of the Electron Transfer Number for the Oxygen Reduction Reaction: From Theory to Experiment. *ACS Catalysis*, *6*(7), 4720-4728. https://doi.org/10.1021/acscatal.6b01581

Zhou, W., Liu, Z., Chen, W., Sun, X., Luo, M., Zhang, X., Li, C., An, Y., Song, S., Wang, K., & Zhang, X. (2023). A Review on Thermal Behaviors and Thermal Management Systems for Supercapacitors. *Batteries*, *9*(2). https://doi.org/10.3390/batteries9020128

BIOGRAPHIES

José L. Sampietro Saquicela, graduated in Electronics, Automation and Control Engineering from the University of the Armed Forces of Ecuador and Master's Degree in Automation and Robotics from the Polytechnic University of Catalonia, Master's Degree in Industrial Organization Engineering from the Polytechnic University of Catalonia. PhD in Automation, Robotics and Advanced Computer Vision at the Polytechnic University of Catalonia (2019).
Email: jose.sampietro@pucese.edu.ec
ORCID: https://orcid.org/0000-0003-0610-089X

Jorge G. Checa Burgos, graduated in Electrical Engineering from the State Technical University of Quevedo (UTEQ) in 2016 and Master's degree in Electricity with a mention in Renewable Energies and Energy Efficiency from the Pontificia Universidad Católica del Ecuador (2024). Teacher and researcher at the Higher Technological Institute City of Valencia.
Email: jorgecheca@itscv.edu.ec
ORCID: https://orcid.org/0000-0001-8322-3872

Raúl C. Ulloa de Souza, graduated in Electrical Engineering from the National Polytechnic School, Master in Electrical Engineering in Distribution from the National Polytechnic School, Master in Business Administration with a Specialty in Project Management from the Prat University of Chile.
Email: raul.ulloa@utelvt.edu.ec
ORCID: https://orcid.org/0000-0003-1885-0161

Jaime R. Bastidas Heredia, specialist in Instrumentation Systems, Automation and Industrial Control, Oil Refineries, Power Generation, Aspen Hysys Expert for the hydrocarbons industry, consultant in the areas of Energy, Electrical Engineering, Electronics and Control for the Hydrocarbons, Renewable Energies, 31 years of experience in Design, construction, assembly, commissioning and maintenance of Control and Control systems Industrial Process Automation and Energy.
Email: Jaime.Bastidas@eppetroecuador.ec
ORCID: https://orcid.org/0000-0003-3022-5756

Luz M. Ávila Pesántez, graduated with a Bachelor's Degree in Secondary Education Sciences in the specialization of Mathematics and Physics at the Central University of Ecuador, Master's Degree in Development of Intelligence and Education at the National University of Chimborazo, Master's Degree in Mathematics with a mention in Modeling and Teaching at the Polytechnic School of Chimborazo, Professor at the Faculty of Business Administration of the Polytechnic School of Chimborazo.
Email: miriam.avila@espoch.edu.ec
ORCID: https://orcid.org/0000-0001-9421-287X

Freddy J. Fares Vargas, graduated in Electrical Engineering with an Industrial specialty from the Polytechnic School of the Litoral, Master's Degree in Industrial Automation and Control from the Polytechnic School of the Litoral, Master's Degree in Business and Business Administration from the State Technical University of Quevedo.
Lecturer at the Higher Technological Institute of the City of Valencia.
Email: freddyfares@itscv.edu.ec
ORCID: https://orcid.org/0000-0003-1400-6676

Leandro A. Bermúdez Herrera, graduated in Electronics and Telecommunications Engineering from the University of the Armed Forces of Ecuador and Master's Degree in Systems and IT Management from the University of the Americas. Professor at Universidad Internacional del Ecuador.

Email: leandro.bermudez@gmail.com
ORCID: https://orcid.org/0009-0002-3590-7166